

Evolution of the Angular Correlation Function

A.J. Connolly, A.S. Szalay and R.J. Brunner

Department of Physics and Astronomy, The Johns Hopkins University, Baltimore, MD
21218

ABSTRACT

For faint photometric surveys our ability to quantify the clustering of galaxies has depended on interpreting the angular correlation function as a function of the limiting magnitude of the data. Due to the broad redshift distribution of galaxies at faint magnitude limits the correlation signal has been extremely difficult to detect and interpret. We introduce a new technique for measuring the evolution of clustering. We utilize photometric redshifts, derived from multicolor surveys, to isolate redshift intervals and calculate the evolution of the amplitude of the angular 2-pt correlation function. Applying these techniques to the the Hubble Deep Field we find that the shape of the correlation function, at $z = 1$, is consistent with a power law with a slope of -0.8 . For $z > 0.4$ the best fit to the data is given by a model of clustering evolution with a comoving $r_0 = 2.37 \text{ h}^{-1} \text{ Mpc}$ and $\epsilon = -0.4^{+0.37}_{-0.65}$, consistent with published measures of the clustering evolution. To match the canonical value of $r_0 = 5.4 \text{ h}^{-1} \text{ Mpc}$, found for the clustering of local galaxies, requires a value of $\epsilon = 2.10^{+0.43}_{-0.64}$ (significantly more than linear evolution). The log likelihood of this latter fit is 4.15 less than that for the $r_0 = 2.37 \text{ h}^{-1} \text{ Mpc}$ model. We, therefore, conclude that the parameterization of the clustering evolution of $(1 + z)^{-(3+\epsilon)}$ is not a particularly good fit to the data.

Subject headings: galaxies: distances and redshifts, galaxies: evolution, large-scale structure of Universe

1. Introduction

The evolution of the clustering of galaxies as a function of redshift provides a sensitive probe of the underlying cosmology and theories of structure formation. In an ideal world we would measure the spatial correlation function of galaxies as a function of redshift and type and use this to compare with the predictions of different galaxy formation theories.

Observationally, however, our ability to efficiently measure galaxy spectra falls rapidly as a function of limiting magnitude and consequently we are limited to deriving spatial statistics from small galaxy samples and at relatively bright magnitude limits (e.g. $I_{AB} < 22.5$, Le Fevre et al. 1996, Carlberg et al. 1997).

To increase the size of the galaxy samples and thereby reduce the shot noise the standard approach has been to measure the angular correlation function, i.e. the projected spatial correlation function (Brainerd et al. 1996, Woods and Fahlman 1997). While this allows us to extend the measure of the clustering of galaxies to fainter magnitude limits ($R < 29$, Villumsen et al. 1997) it has an associated limitation. For a given magnitude limit the amplitude of the angular correlation function is sensitive to the width of the galaxy redshift distribution, $N(z)$. At faint magnitude limits $N(z)$ is very broad and consequently the clustering signal is diluted due to the large number of randomly projected pairs.

In this letter we introduce a new approach for quantifying the evolution of the angular correlation function; we apply photometric redshifts (Connolly et al. 1995, Lanzetta et al. 1996, Gwyn and Hartwick 1996, Sawicki et al. 1997) to isolate particular redshift intervals. In so doing we can remove much of the foreground and background contamination of galaxies and measure an amplified angular clustering. We discuss here the particular application of this technique to the Hubble Deep Field (HDF; Williams et al. 1996).

2. The Photometric Catalog

From version 2 of the “drizzled” HDF images (Fruchter and Hook 1996) we construct a photometric catalog, in the U_{300} , B_{450} , V_{606} and I_{814} photometric passbands, using the SExtractor image detection and analysis package of Bertin and Arnout (1996). Object detection was performed on the I_{814} images using a 1 arcsec detection kernel. For those galaxies with $I_{814} < 27$ we measure magnitudes in all four bands using a 2 arcsec diameter aperture magnitude. The final catalog comprises 926 galaxies and covers ~ 5 sq arcmin.

From these data we construct a photometric redshift catalog. For $I_{814} < 24$, we apply the techniques of Connolly et al. (1995, 1997), i.e. we calibrate the photometric redshifts using a training set of galaxies with known redshift. For fainter magnitudes ($24 < I_{814} < 27$) we estimate the redshifts by fitting empirical spectral energy distributions (Coleman et al. 1980) to the observed colors (Gwyn and Hartwick 1996, Lanzetta et al. 1996 and Sawicki et al. 1997). A comparison between the predicted and observed redshifts shows the photometric redshift relation has an intrinsic dispersion of $\sigma_z \sim 0.1$.

3. The Angular Correlation function

We calculate the angular correlation function, $w(\theta)$, using the estimator derived by Landy and Szalay (1993),

$$w(\theta) = \frac{DD - 2DR + RR}{RR}, \quad (1)$$

where DD and RR are the autocorrelation function of the data and random points respectively and DR is the cross-correlation between the data and random points. In the limit of weak clustering this statistic is the 2-point realization of a more general representation of edge-corrected n-point correlation functions (Szapudi and Szalay 1997). As such it provides an optimal estimator for the HDF where the small field-of-view makes the corrections for the survey geometry significant.

We calculate $w(\theta)$ between 1 and 220 arcsec with logarithmic binning. In the subsequent analysis we impose a lower limit of 3 arcsec to remove any artificial correlations due to the possibility that the image analysis routines may decompose a single galaxy image into multiple detections (at $z = 1$ this corresponds to $12 \text{ h}^{-1} \text{ kpc}$ for $q_o = 0.5$). For the random realizations we construct a catalog of 10000 points (approximately 50 times the number of galaxies per redshift interval) with the same geometry as the photometric data. To account for the small angular size of the HDF we apply an integral constraint assuming that the form of $w(\theta)$ is given by a power law with a slope of -0.8 .

Errors are estimated assuming Poisson statistics. The expected uncertainty in each bin is calculated from the number of random pairs (when scaled to the number of data points). Over the range of angles for which we calculate the correlation function errors derived from Poisson statistics are comparable to those from bootstrap resampling (Villumsen et al. 1997).

3.1. The Angular Correlation Function in the HDF

In Figure 1a we show the angular correlation function of the full $I_{814} < 27$ galaxy sample (filled triangles). The error bars represent one sigma errors. The amplitude of the correlation function is comparable to that found by Villumsen et al. (1997) for an R selected galaxy sample in the HDF. It is consistent with a positive detection of a correlation signal at the 2σ significance level. Superimposed on this figure is the correlation function for those galaxies with $1.0 < z < 1.2$ (filled squares). Isolating this particular redshift interval the amplitude of the correlation function is amplified by approximately a factor of ten.

If we parameterize the angular correlation function as a power law with $w(\theta) = A_w \theta^{1-\gamma}$

then, from Limber’s equations (Limber 1954), we can estimate how the amplitude, A_w , should scale as a function of redshift and width of the redshift distribution,

$$A_w = \sqrt{\pi} \frac{\Gamma[(\gamma - 1)/2]}{\Gamma[\gamma/2]} r_0^\gamma \frac{\int_0^\infty dz N(z)^2 (1+z)^{-(3+\epsilon)} x(z)^{1-\gamma} g(z)}{\left[\int_0^\infty N(z) dz\right]^{-2}} \quad (2)$$

where,

$$x(z) = 2 \frac{((\Omega - 2)(\sqrt{1 + \Omega z} - 1) + \Omega z)}{\Omega^2 (1 + z)^2}, \quad (3)$$

is the comoving angular diameter distance,

$$g(z) = (1 + z)^2 \sqrt{1 + \Omega z}, \quad (4)$$

$N(z)$ is the redshift distribution and ϵ represents a parameterization of the evolution of the spatial correlation function (see below).

For a normalized Gaussian redshift distribution, centered at \bar{z} , with $\bar{z} \gg 0$ and dispersion σ_z , A_w is proportional to $1/\sigma_z$. Therefore, the amplitude of the angular correlation function should be inversely proportional to the width of the redshift distribution over which it is averaged. In Figure 1 if we assume that the magnitude limited sample ($I_{814} < 27$) has a mean redshift of $z = 1.1$ and a dispersion of $\Delta z = 0.5$ (consistent with the derived photometric redshift distribution) then isolating the redshift interval $1.0 < z < 1.2$ should result in an amplification of a factor of 5 in the correlation function (comparable to that which we detect).

3.2. The Angular correlation function as a function of redshift

A limitation on studying large-scale clustering with the HDF is its small field of view. For $\Omega = 1$, the 220 arcsec maximal extent of the WFPC2 images corresponds to $0.7 \text{ h}^{-1} \text{ Mpc}$ and $0.9 \text{ h}^{-1} \text{ Mpc}$ at redshifts of $z = 0.4$ and $z = 1.0$ respectively. Isolating very narrow intervals in redshift (e.g. binning on scales of $\sigma_z < 0.1$, the intrinsic dispersion in the photometric-redshift relation) can, therefore, result in the correlation function being dominated by a single structure, e.g. a cluster of galaxies. To minimize the effect of the inhomogeneous redshift distribution observed in the HDF (Cohen et al. 1996) we divide the HDF sample into bins of width $\Delta z = 0.4$ based on their photometric redshifts.

For each redshift interval, $0.0 < z < 0.4$, $0.4 < z < 0.8$, $0.8 < z < 1.2$ and $1.2 < z < 1.6$, we fit the observed correlation function, with a power law with a slope of -0.8 , over the range $3 < \theta < 220$ arcsec. From this fit we measure the amplitude of the correlation function at a fiducial scale of 10 arcsec. The choice of this particular angle is simply a

convenience as it is well sampled at all redshift intervals. In Figure 2 we show the evolution of the amplitude as a function of redshift. For redshifts $z > 0.4$ the relation is relatively flat with a mean value of 0.12. At $z < 0.4$ we would expect the amplitude to rise rapidly with redshift due to the angular diameter distance relation. We find, however, that the amplitude remains flat even for the lowest redshift bin. This implies that there is a bias in the clustering signal inferred from the $0.0 < z < 0.4$ redshift interval (see Section 4).

The value of the correlation function amplitude is comparable to those derived from deep magnitude limited samples of galaxies. Hudon and Lilly (1997) find an amplitude, measured at 1 degree, of $\log A_w = -2.68 \pm 0.08$ for an $R < 23.5$ galaxy sample. Woods and Fahlman for a somewhat deeper survey, $R < 24$, derive a value of -2.94 ± 0.06 . At these magnitude limits the mean redshift is approximately 0.56 (Hudon and Lilly, 1997) and the width is comparable to the redshift intervals of $\Delta z = 0.4$ that we apply to the HDF data. Therefore, our measured amplitude of -2.92 ± 0.06 is in good agreement with these previous results.

4. Modeling the Clustering Evolution

We parameterize the redshift evolution of the spatial correlation function as $(1+z)^{-(3+\epsilon)}$, where values of $\epsilon = -1.2$, $\epsilon = 0.0$ and $\epsilon = 0.8$ correspond to a constant clustering amplitude in comoving coordinates, constant clustering in proper coordinates and linear growth of clustering respectively (Peebles 1980). From Equation 2 we construct the expected evolution of the amplitude of the angular correlation function, projected to 10 arcsec, for a range of values of r_0 , ϵ and Ω . We assume that the intrinsic uncertainty of the photometric redshift for each galaxy can be approximated by a Gaussian distribution, with a dispersion $\sigma_z = 0.1$ (consistent with observations), and determine the $N(z)$ within a particular redshift interval as being composed of a sum of these Gaussian distributions.

In Figure 2 we illustrate the form of this evolution for two sets of models, one with $r_0 = 5.4 \text{ h}^{-1} \text{ Mpc}$ and the second with $r_0 = 2.37 \text{ h}^{-1} \text{ Mpc}$ (the best fit to the data). For each model we assume $\Omega = 1$ and plot the evolutionary tracks for $\epsilon = -1.2$ (solid line), $\epsilon = 0.0$ (dotted line) and $\epsilon = 0.8$ (dashed line). For $z > 0.4$ and a low r_0 the observed amplitude of the correlation function is well matched by that of the predicted evolution. For redshifts $z < 0.4$ the observed clustering is approximately a factor of three below the $r_0 = 2.37 \text{ h}^{-1} \text{ Mpc}$ model.

This is not unexpected given the selection criteria for the HDF. The field was chosen to avoid bright galaxies visible on a POSS II photographic plate. This corresponds to

a lower limit for the HDF photometric sample of $F814W \sim 20$ (Marc Postman, private communication). The redshift distribution for an $I_{814} < 20$ magnitude limited sample has a median value of $z = 0.25$ and a width of approximately $\Delta z = 0.25$ (Lilly et al. 1995). Therefore, by excluding the bright galaxies within the HDF we artificially suppress the clustering amplitude in the redshift range $0.0 < z < 0.5$. We can expect, as we have found, that the first redshift bin in the HDF will significantly underestimate the true clustering signal. Those redshifts bins at $z > 0.5$ are unlikely to be significantly affected by this magnitude limit.

To constrain the models for the clustering evolution we, therefore, exclude the lowest redshift point in our sample, i.e. $0.0 < z < 0.4$, and determine the goodness-of-fit of each model using a χ^2 statistic. The three dimensional χ^2 distribution was derived for the phase space given by $1 < r_0 < 5 \text{ h}^{-1} \text{ Mpc}$, $-4 < \epsilon < 4$ and $0.2 < \Omega < 1$. We find that ϵ is relatively insensitive to the value of Ω with a variation of typically 0.4 for the range $0.2 < \Omega < 1.0$. As this is small when compared to the intrinsic uncertainty in measuring ϵ we integrated the probability distribution over all values of Ω .

In Figure 3a we show the range of possible values for ϵ as a function of r_0 . The errorbars represent the 95% confidence intervals derived from the integrated probability distribution. Figure 3b shows the log likelihood for these fits as a function of r_0 . The HDF data are best fitted by a model with a comoving $r_0 = 2.37 \text{ h}^{-1} \text{ Mpc}$ and $\epsilon = -0.4^{+0.37}_{-0.65}$. The value of r_0 is comparable to recent spectroscopic and photometric surveys with Hudon and Lilly (1996) finding $r_0 = 2.75 \pm 0.64 \text{ h}^{-1} \text{ Mpc}$ and Le Févre et al. (1996) $r_0 = 2.03 \pm 0.14 \text{ h}^{-1} \text{ Mpc}$.

Given our redshift range, the I-band selected HDF data are comparable to a sample of galaxies selected in the restframe U ($z = 1.4$) through V ($z = 0.6$). To tie these observations into the clustering of local galaxies we, therefore, compare our results with the B band selected clustering analysis of Davis and Peebles (1983) and Loveday et al. (1992). Assuming a canonical value of $r_0 = 5.4 \text{ h}^{-1} \text{ Mpc}$ we require $\epsilon = 2.10^{+0.43}_{-0.64}$ to match the high redshift HDF data (i.e. significantly more evolution than that predicted by linear theory).

A bias may be introduced into the analysis of the clustering evolution due to the fact that the I band magnitude selection corresponds to a selection function that is redshift dependent (see above). If, as is observed in the local Universe, the clustering length is dependent on galaxy type then selecting different inherent populations may mimic the observed clustering evolution. To determine the effect of this bias we allow r_0 to be a function of redshift (with r_0 varying by $2 \text{ h}^{-1} \text{ Mpc}$ from $z = 0$ to $z = 2$). The magnitude of this change in r_0 is consistent with the morphological dependence of r_0 observed locally (Loveday et al. 1995, Iovino et al. 1993). Allowing for this redshift dependence reduces the

value of ϵ by approximately 0.5 for all values of r_0 (e.g. for $r_0 = 5.4 \text{ h}^{-1} \text{ Mpc}$ $\epsilon = 1.6_{-0.64}^{+0.43}$).

It is worth noting that even with these large values of ϵ and accounting for the bias due to the I band selection the evolution of the clustering in the HDF is better fitted by a low value of r_0 (the log likelihood is 4.15 less than the fit to $r_0 = 2.37 \text{ h}^{-1} \text{ Mpc}$). Parameterising the evolution of galaxy clustering is, therefore, not particularly well represented by the form $(1+z)^{-(3+\epsilon)}$ and it may be better for future studies to discuss the evolution in terms of the amplitude at a particular comoving scale rather than r_0 and ϵ .

5. Conclusions

Photometric redshifts provide a simple statistical means of directly measuring the evolution of the clustering of galaxies. By isolating narrow intervals in redshift space we can reduce the number of randomly projected pairs and detect the clustering signal to high redshift and faint magnitude limits. Applying these techniques to the HDF we can characterize the evolution of the angular 2 pt correlation function out to $z = 1.6$. For redshifts $0.4 < z < 1.6$ we find that the amplitude of the angular correlation function is best parameterized by a comoving $r_0 = 2.37 \text{ h}^{-1} \text{ Mpc}$ and $\epsilon = -0.4_{-0.65}^{+0.37}$. To match, however, the canonical local value for the clustering length, $r_0 = 5.4 \text{ h}^{-1} \text{ Mpc}$, requires $\epsilon = 2.1_{-0.6}^{+0.4}$, significantly more than simple linear growth.

It must be noted that while these results are in good agreement with those from published photometric and spectroscopic surveys (Le Fèvre et al 1996, Hudon and Lilly 1996) there are two caveats that should be considered before applying them to constrain models of structure formation. The small angular extent of the HDF (at a redshift, $z = 1$, the field-of-view of the HDF is approximately $0.9 \text{ h}^{-1} \text{ Mpc}$) means that fluctuations on scales larger than we probe will contribute to the variance of the measured clustering (Szapudi and Colombi 1996). Secondly, the requirement that the HDF be positioned such that it avoids bright galaxies ($I_{814} < 20$) biases our clustering statistics by artificially suppressing the number of low redshift galaxies (a bias that will be present in most deep photometric surveys). Therefore, the clustering evolution in the HDF may not necessarily be representative of the general field population. Given this, there is enormous potential for the application of this technique to systematic wide angle multicolor surveys, such as the Sloan Digital Sky Survey,

We would like to thank Marc Postman and Mark Dickinson for helpful comments on the selection and interpretation of the Hubble Deep Field data. We acknowledge partial support from NASA grants AR-06394.01-95A and AR-06337.11-94A (AJC) and an LTSA

grant (ASZ).

REFERENCES

Bertin, E., & Arnouts, S. 1996, *A&A*, 117, 393

Brainerd, T.G., Blandford, R.D. & Smail, I., 1996, *ApJ*, 466, 623

Carlberg, R.G., Cowie, L.L., Songalia, A., Hu & E.M., 1997, *ApJ*, 484, 538

Coleman, G.D., Wu, C.-C. & Weedman, D.W., 1980, *ApJS*, 43, 393

Connolly, A.J., Csabai, I., Szalay, A.S., Koo, D.C., Kron, R.G. & Munn, J.A., 1995, *AJ* 110, 2655

Connolly, A.J., Szalay, A.S., Dickinson, M.E., SubbaRao, M.U. & Brunner, R.J., 1997, *ApJ* 486, L11

Cohen, J.G., Cowie, L.L., Hogg, D.W., Songaila, A., Blandford, R., Hu, E.M. & Shopbell, P., 1996, *ApJ*, 471, L5

Davis, M. & Peebles, P.J.E., 1983, *ApJ*, 267, 465

Fisher, K.B., Davis, M., Strauss, M.A., Yahil, A. & Huchra, J., 1994, *MNRAS*, 266, 50

Fruchter, A.S. & Hook, R.N., 1997, <http://www.stsci.edu/~fruchter/dither/drizzle.html>

Gwyn, S.D.J. & Hartwick, F.D.A., 1996, *ApJ*, 468, L77

Hudon, J.D. & Lilly, S.J., 1996, *ApJ*, 469, 519

Iovino, A., Giovanelli, R., Haynes, M., Chincarini, G & Guzzo, L., 1993, *MNRAS*, 265, 21

Landy, S.D. & Szalay, A.S., 1993, *ApJ*, 412, 64

Lanzetta, K.M., Yahil, A. & Fernández-Soto, A., 1996, *Nature*, 381, 759

Le Fèvre, O., Hudon, D., Lilly, S.J., Crampton, D., Hammer, F., 1996, *ApJ*, 461, 534

Lilly, S.J., Le Fevre, O., Crampton, D., Hammer, F., Tresse, L., 1995, *ApJ*, 455, 50

Limber, D.N., 1954, *ApJ*, 119, 655

Loveday, J., Peterson, B.A., Efstathiou, G. & Maddox, S.J., 1992, *ApJ*, 390, 338

Loveday, J., Maddox, S.J., Efstathiou, G. & Peterson, B.A., 1995, *ApJ*, 442, 457

Peebles, P.J.E., 1980, “The Large-Scale Structure of the Universe”, (Princeton: Princeton University Press)

Sawicki, M.J., Lin, H. & Yee, H.K.C., 1997, *AJ*, 113, 1

Szapudi, I. & Colombi, S., 1996, *ApJ*, 470, 131

Szapudi, I. & Szalay, A.S., 1998, ApJ, 494, L41
Villumsen, J.V., Freudling, W. & Da Costa, L.N., 1997, ApJ 481, 578
Woods, D. & Fahlman, G.G., 1997, ApJ, 490, 11
Williams, R.E. et al., 1996, AJ, 112, 1335

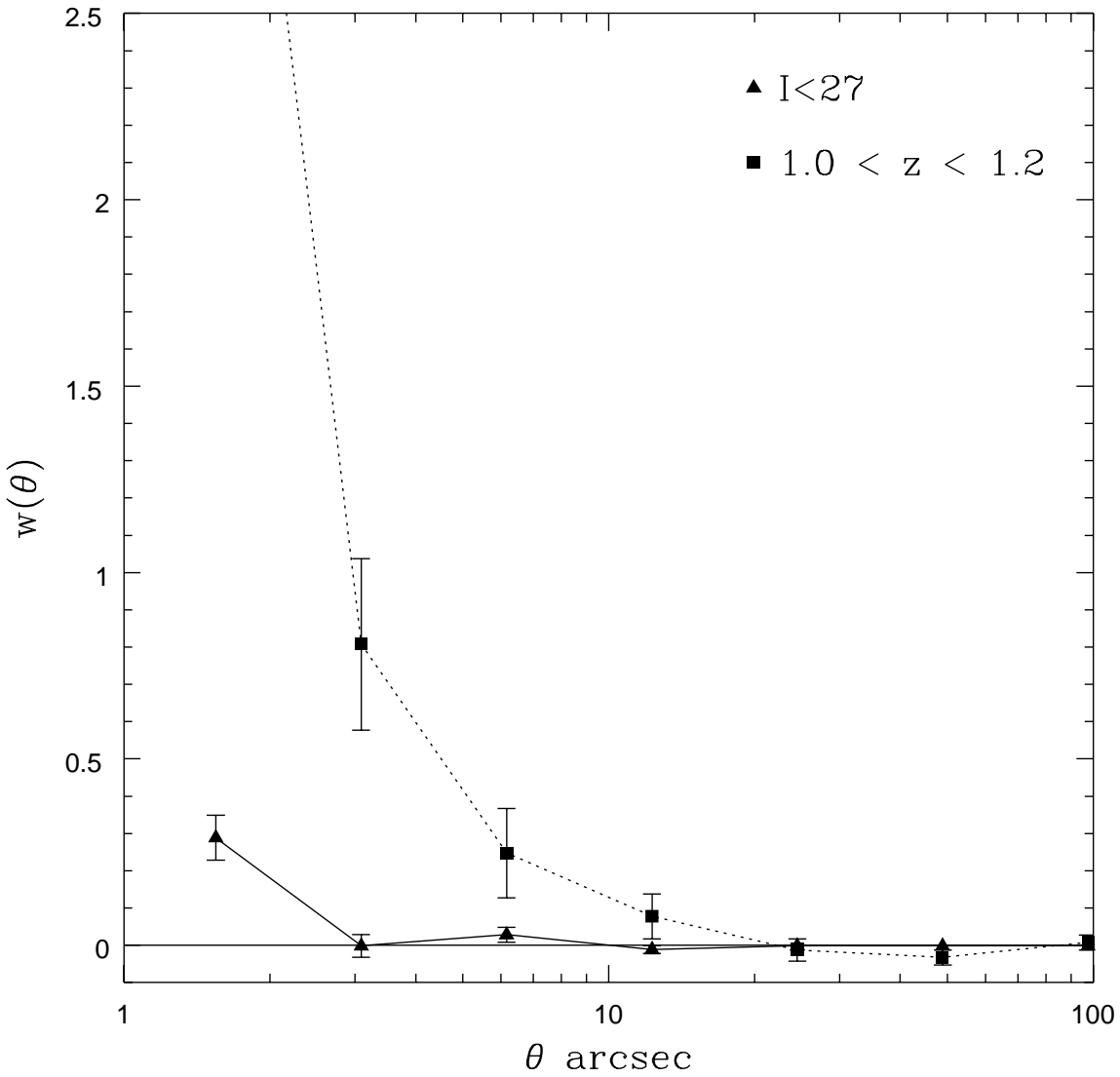


Fig. 1.— The 2-pt angular correlation function for galaxies within the HDF with $I_{814} < 27$. The triangles represent the correlation function for a magnitude limited sample. The statistical significance of a positive detection is approximately 2σ . The squares show the correlation function if we isolate, using photometric redshifts, a subset of galaxies within the redshift interval $1.0 < z < 1.2$. The amplification of the signal due to the reduction in the number of projected random pairs is approximately a factor of 10.

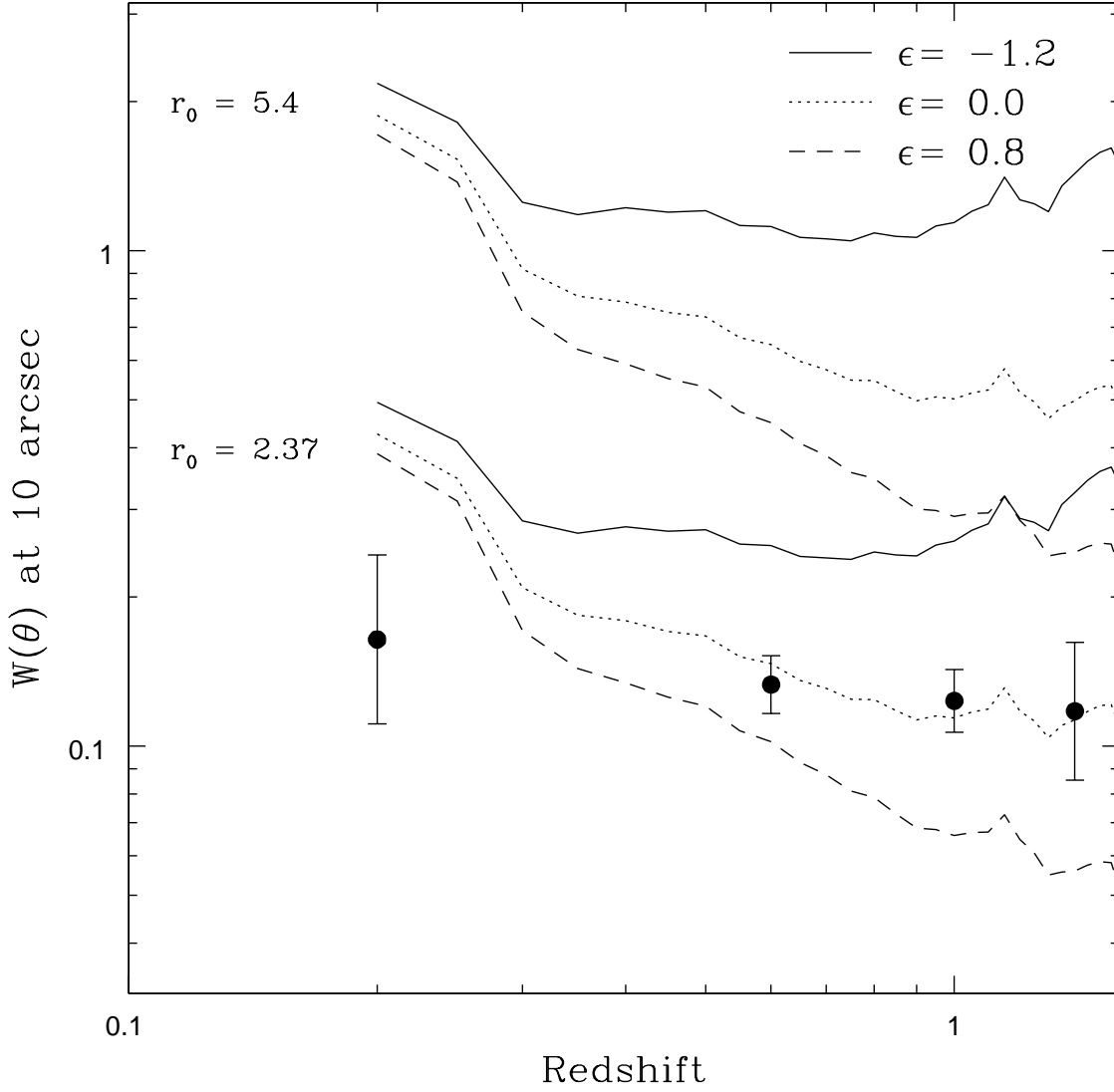


Fig. 2.— Evolution of the amplitude of the angular correlation function (measured at 10 arcsec) as a function of redshift. Each point is measured within a redshift interval of $\Delta z = 0.4$. The exact $N(z)$ for these intervals is constructed from the photometric redshift distribution by assuming the error distribution for a photometric redshift can be approximated by a Gaussian with a dispersion of $\sigma_z = 0.1$. We illustrate the expected evolution of the correlation function amplitude for two sets of models, one with $r_0 = 2.37 \text{ h}^{-1} \text{ Mpc}$ (the best fit to the data) and a second with $r_0 = 5.4 \text{ h}^{-1} \text{ Mpc}$ (the canonical value for local observations). For each value of r_0 we give the evolution for $\epsilon = -1.2$ (fixed clustering in comoving coordinates; solid line), $\epsilon = 0.0$ (fixed clustering in proper coordinates; dotted line) and $\epsilon = 0.8$ (linear evolution of clustering; dashed line).

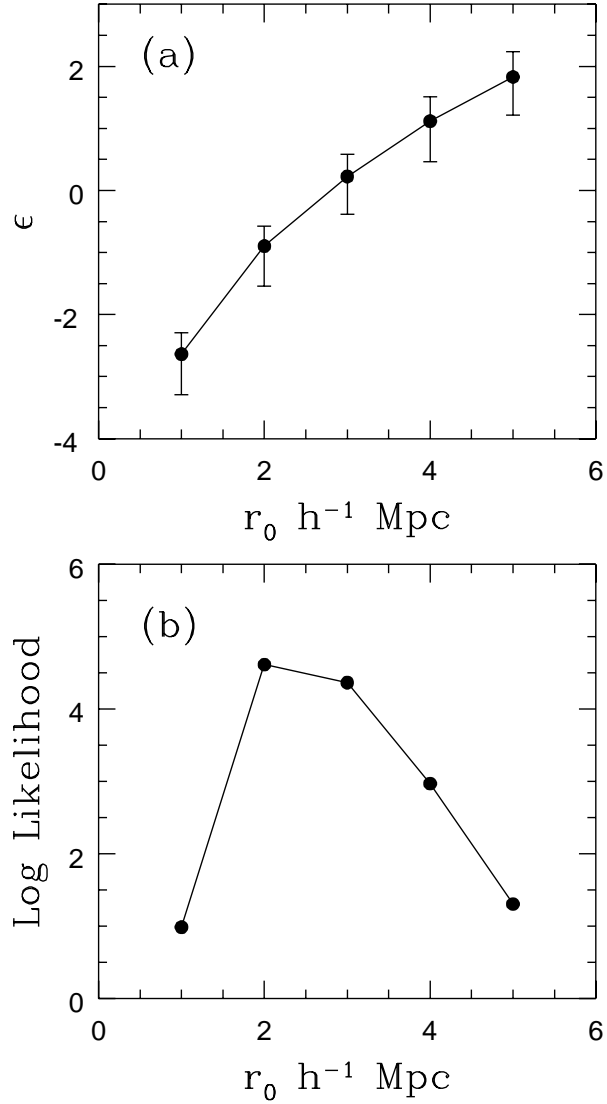


Fig. 3.— (a) Integrating the probability distribution for the value of ϵ at a given r_0 over all values of $0.2 < \Omega < 1.0$ we can estimate the range of values of ϵ that best fit the HDF data. For each value of r_0 within the range $1 < r_0 < 5 \text{ } h^{-1} \text{ Mpc}$ we give the best fit for ϵ and the 95% probability error bars. To fit the local value of $r_0 = 5.4 \text{ } h^{-1} \text{ Mpc}$ requires an $\epsilon = 2.1^{+0.4}_{-0.6}$, significantly more than linear evolution. (b) The log likelihood for the best fit for ϵ , at a given r_0 . The best fit to the data is given by an $r_0 = 2.37 \text{ } h^{-1} \text{ Mpc}$. The fit to $r_0 = 5.4 \text{ } h^{-1} \text{ Mpc}$ has a log likelihood 4.15 less than that for $r_0 = 2.37 \text{ } h^{-1} \text{ Mpc}$.